Electronic Supplementary Material (ESI) for New Journal of Chemistry.
This journal is © The Royal Society of Chemistry and the Centre National de la Recherche Scientifique 2022

Electronic Supplementary Information

Insights into self-aggregating properties of a solvatochromic probe and interaction with β-lactoglobulin

Sagnik De and Gopal Das*

Department of Chemistry, Indian Institute of Technology Guwahati, Assam 781039, India.

Fax: + 91 361 258 2349; Tel: +91 361258 2313; E-mail: gdas@iitg.ac.in

General Methods and Materials

All reagents, starting materials, solvents, and protein samples were procured from commercial sources and used without further purification. . The absorption and emission spectral studies were measured in a Perkin-Elmer Lamda-750 UV-Vis spectrophotometer and Horiba Fluoromax-4 spectrofluorometer respectively. Recording of UV-vis spectra was done in 10 mm path length quartz cuvettes in the range 300-700 nm wavelength, while fluorescence measurement was done using a 10 mm path length quartz cuvette with a slit width of 3 nm at 25 °C. Chemical shifts of NMR were recorded using a BRUKER-500 MHz and a BRUKER-600 MHz instrument, and reported on a scale in parts per million (ppm). Spin multiplicities from ^{1}H NMR spectra were described using the following abbreviations: s = singlet; d = doublet; t = triplet; m = multiplet. IR spectra with 4000-400 cm^{-1} range were collected using a Perkin Elmer-Spectrum AT-IR spectrometer. Atomic Force Microscope (Make: Oxford, Model: Cypher) and Field Emission Scanning Electron Microscope(Make: Zeiss, Model:-Sigma 300) were used to characterize the topographical and morphological details.

Detection Limit

From the fluorescence titration profile, the detection limits were obtained. In this calculation, to obtain the standard deviation(σ) of blank measurement, the fluorescence emission spectrum of the probe as well as the ensemble were measured 10 times. In the case of slope determination, the ratio of the fluorescence emission at a certain wavelength was plotted against the concentration of the guest analyte. The equation used for deducting the detection limit is as follows:

Detection limit = $3\sigma/k$ (1)[1-2]

Where, σ = standard deviation of blank measurement,

k = slope between the ratio of fluorescence emission vs corresponding guest concentration

Field Emission Scanning Electron Microscope

FESEM imaging studies were conducted separately with a solution of $\mathbf{L_1}$ (1 mM) and $\mathbf{L_2}$ (1 mM) by changing water fraction from 0% to 100% in MeOH-H_2O by drop (2 μl) cast method on glass plates covered with Al-foil using Gemini 300 FESEM (Carl Zeiss).

Atomic Force Microscopy

Transformations of $\mathbf{L_1}$ due to solvent switching were observed from a drop-cast solution of $\mathbf{L_1}$ (10 μM) in a MeOH-water medium using Asylum Research Cypher (Oxford Instruments).

Dynamic light scattering studies

The particle sizes of $\mathbf{L_1}$ and $\mathbf{L_2}$, aggregated states were measured by dynamic light scattering (DLS) experiments on Malvern Zetasizer Nano ZS instrument equipped with a 4.0 mW He–Ne laser operating at a wavelength of 633 nm. The samples and the background were measured at room temperature (25 °C). DLS experiments were carried out with optically clear solutions of $\mathbf{L_1}$ and $\mathbf{L_2}$ (10 μM) to observe the change in the particle size upon increasing the MeOH fraction. The solution was equilibrated for 60 minutes before taking the measurements.

Density Functional Theory (DFT) Study

DFT optimizations of $\mathbf{L_1}$ and $\mathbf{L_2}$ were carried out with the RB3LYP/ 6-31G method basis set using the Gaussian 09 program where the calculated total energy is **-1313.63550213 a.u.** and **-1232.09637024 a.u** respectively.

Circular dichroism measurements

CD spectra of aqueous solutions of $\mathbf{L_1}$ and $\mathbf{L_2}$ (0.5 μM), only βlg (10 μg/mL) and βlg in presence of $\mathbf{L_1}$ and $\mathbf{L_2}$ were recorded by using a quartz cuvette of 10 mm path length with a J-1500 (Jasco) spectropolarimeter at room temperature. Spectra were collected at 1 nm intervals and 1 nm bandwidth from 190 to 240 nm.

Molecular Docking

Molecular docking was computed to examine the energetically and geometrically stable conformation of probe $\mathbf{L_1}$ bound to βlg. AutoDockTools-1.5.6 was used to generate a docked conformation of $\mathbf{L_1}$ with βlg by employing a Genetic Algorithm (GA) and a Lamarckian Genetic Algorithm. The binding sites and binding free energies of $\mathbf{L_1}$ within the active site of βlg were studied by this software. The crystal structure of βlg (10.2210/pdb3NPO/pdb) was retrieved from the PDB bank and subjected to energy refinement, hydrogen additions, and solvent removal through Swiss PDB Viewer v.4.1.0 to allow all the residues to adopt a correct and stable configuration. To define all binding sites, a grid box was generated with a

spacing of 0.375 Å and dimensions of (60×60×60) points (.gpf file). The docking parameters were inserted as the number of GA runs was 25. The output is selected as Lamarckian GA (.dpf file), which was applied in AutoDockTools-1.5.6 to conduct docking simulations. Energy minimization and optimization of the probe $\mathbf{L_1}$ were also performed. In the end, analysis of the docking result of the probe $\mathbf{L_1}$ was done using BIOVIA discovery studio 2021 viewer programs, and the docking structure with the lowest binding energy calculated by AutoDockTools-1.5.6 was selected as the best binding conformation.

Preparation of simulated fluid mediums

Simulated Gastric fluid, Artificial body fluid, and Simulated Intestinal fluid were provided by the Department of Biosciences and Bioengineering, IIT Guwahati. The composition for simulated body fluid was 8.035 g/L of NaCl, 0.355 g/L of $NaHCO_3$, 0.225 g/L of KCl, 0.231 g/L of $K_2HPO_4{\cdot}3H_2O$, 0.311 g/L of $MgCl_2{\cdot}6H_2O$, 0.292 g/mL $CaCl_2$, 0.072 g/L of Na_2SO_4, 6.110 g/L of Tris-hydoxymethyl aminomethane. The composition for simulated gastric fluid was 3 g/L of Pepsin, 0.5 % w/v of sterile saline and adjusted to pH=2. The composition for simulated intestinal fluid was 0.1 % w/v of pancreatin, 0.5 % w/v of saline, adjusted to pH=8.0. The composition for simulated urine has been prepared by reported protocol.

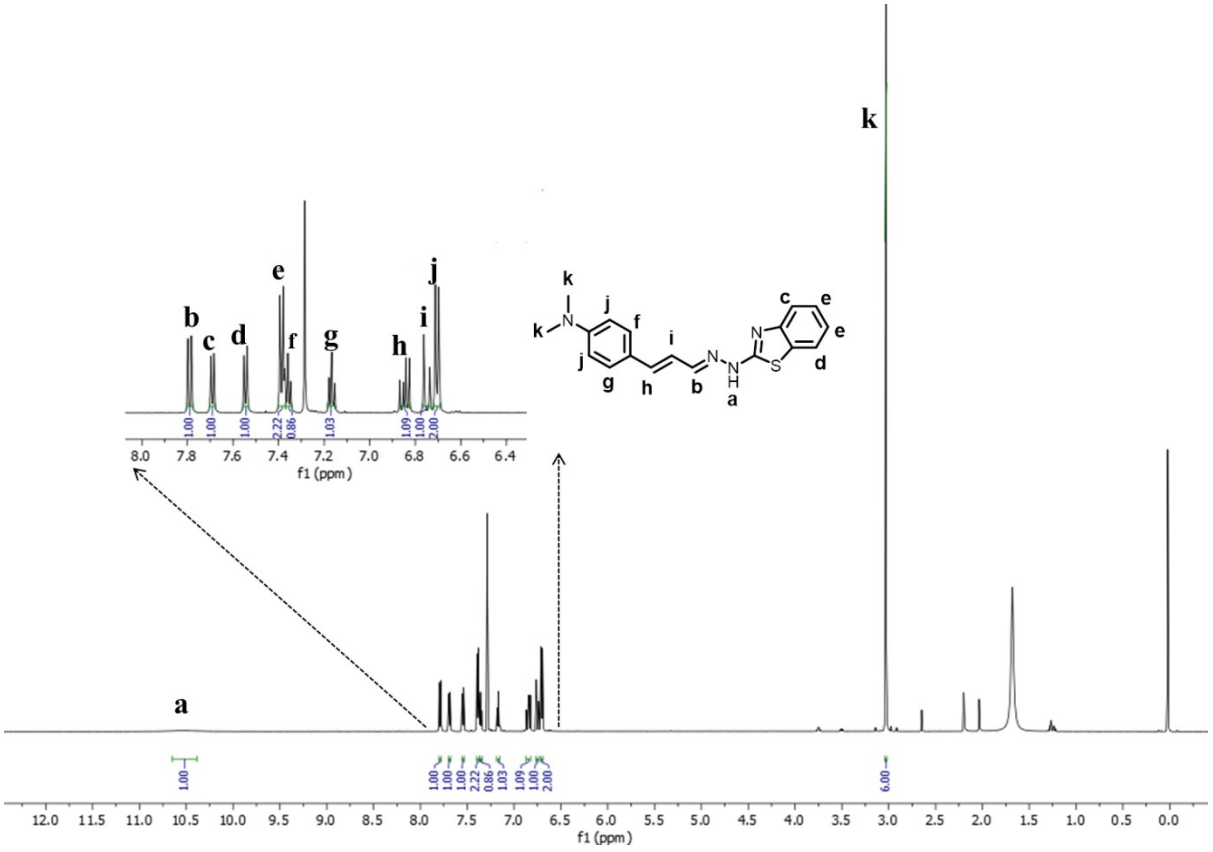

Figure S1: ^{1}HNMR of $\mathbf{L_1}$ in $CDCl_3$ at room temperature.

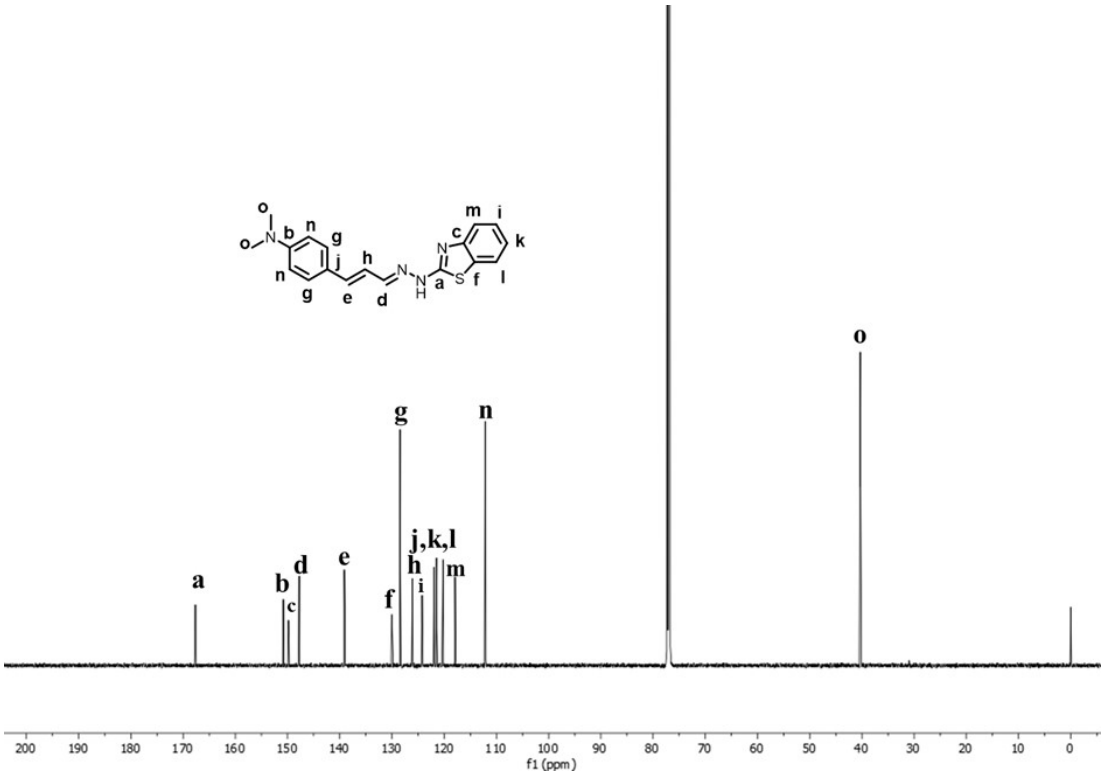

Figure S2: ^{13}CNMR of $\mathbf{L_1}$ in $CDCl_3$ at room temperature.

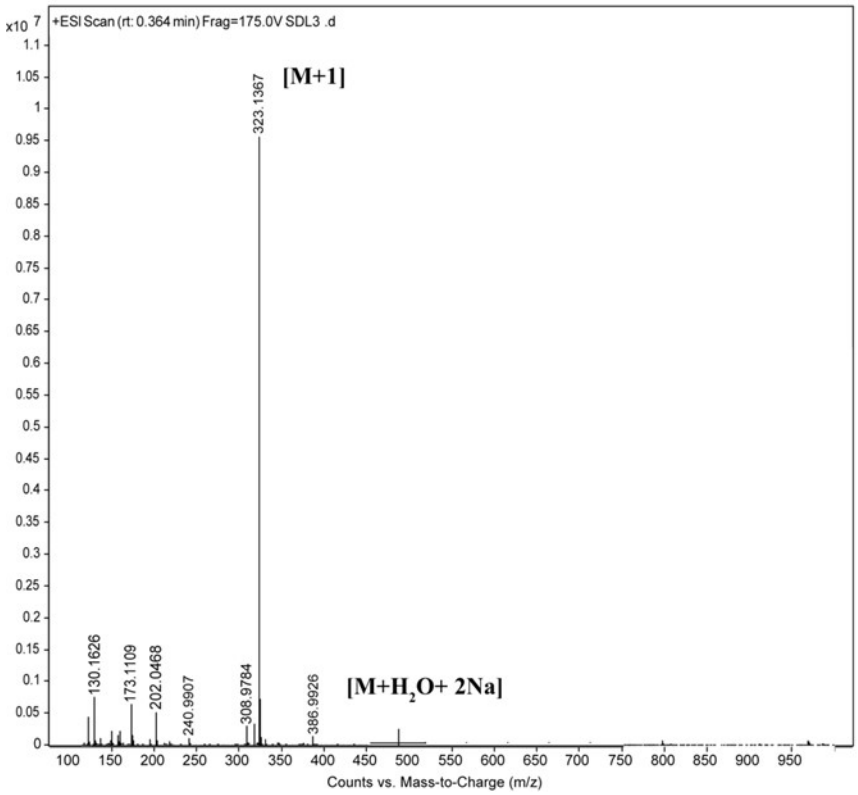

Figure S3: Mass spectra of $\mathbf{L_1}$.

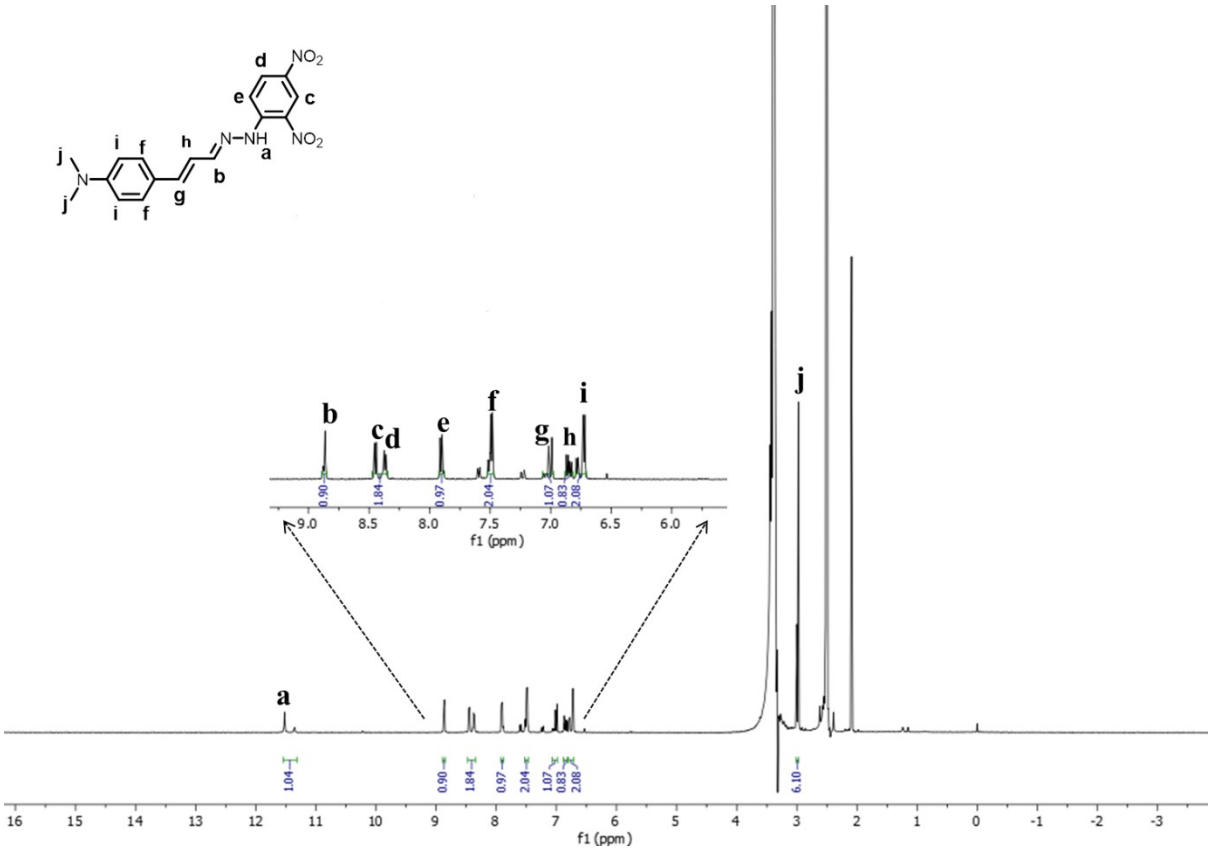

Figure S4: ^{1}HNMR of $\mathbf{L_2}$ in DMSO-d6 at room temperature.

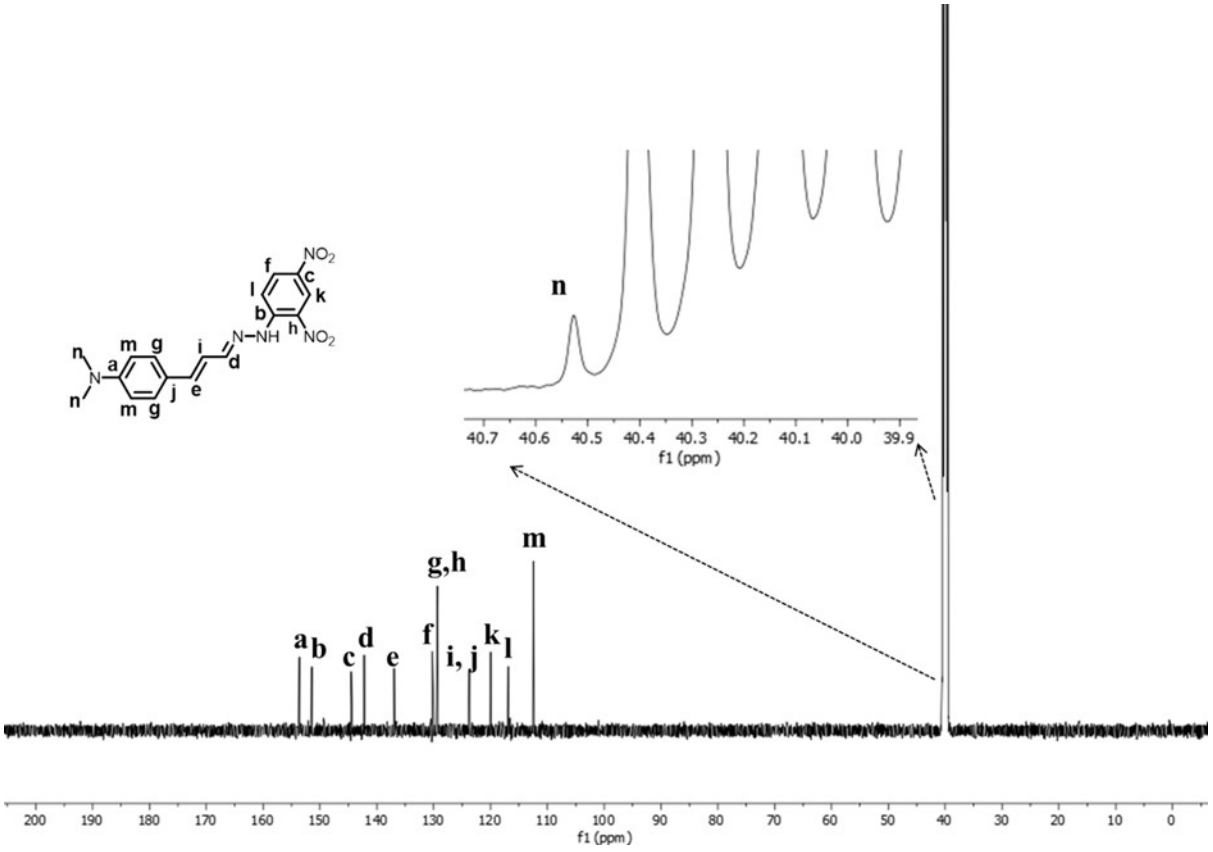

Figure S5: ^{13}CNMR of $\mathbf{L_2}$ in DMSO-d6 at room temperature.

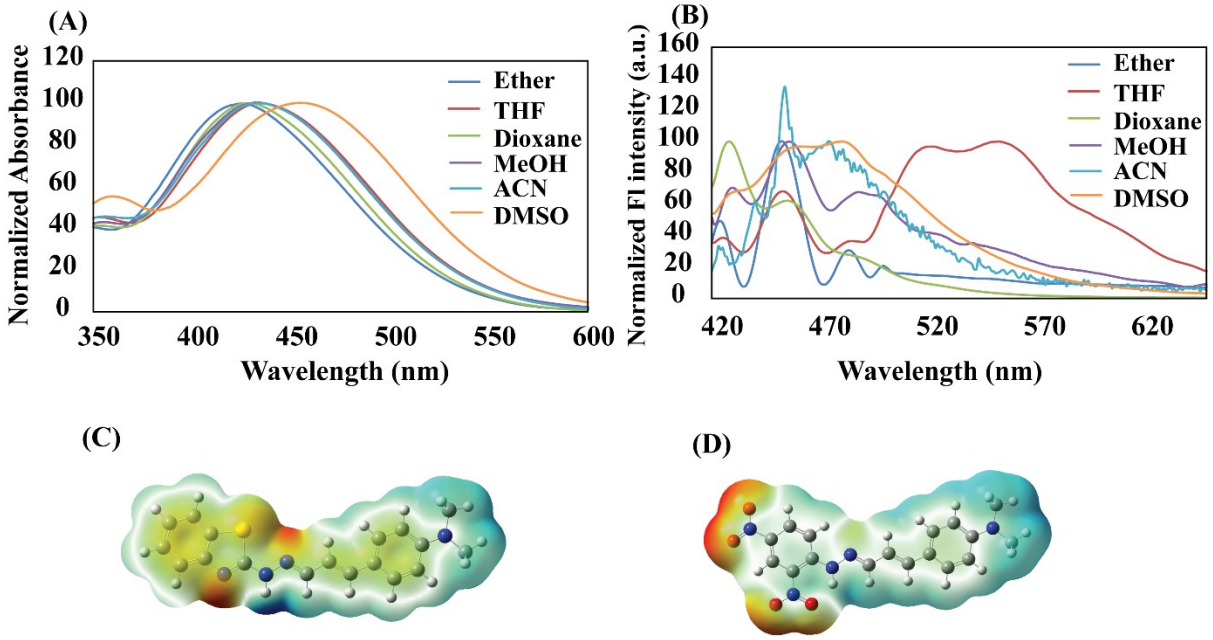

Figure S6: (A) Absorption spectra of $\mathbf{L_2}$ (10 μM) with varying solvents (B) Emission spectra of $\mathbf{L_2}$ (10 μM) with varying solvents (C) MEP diagram of $\mathbf{L_1}$ (D) MEP diagram of $\mathbf{L_2}$.

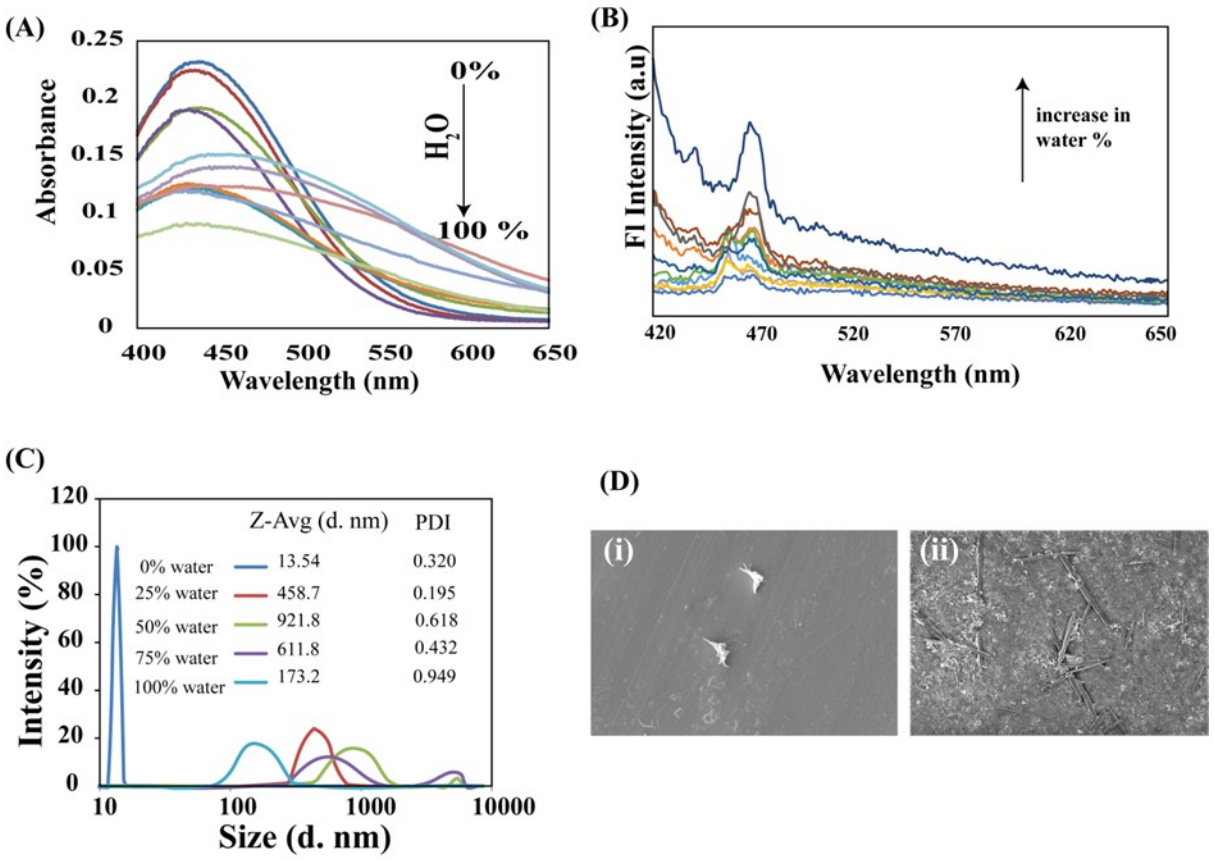

Figure S7: (A) Absorption spectra of $\mathbf{L_2}$ (10 μM) with varying MeOH-water percentage (B) Emission spectra of $\mathbf{L_2}$ (10 μM) with varying MeOH-water percentage (C) Output of DLS experiment of $\mathbf{L_2}$. (D) FESEM images of $\mathbf{L_2}$ in (i) 100 % MeOH and (ii) 100% Water.

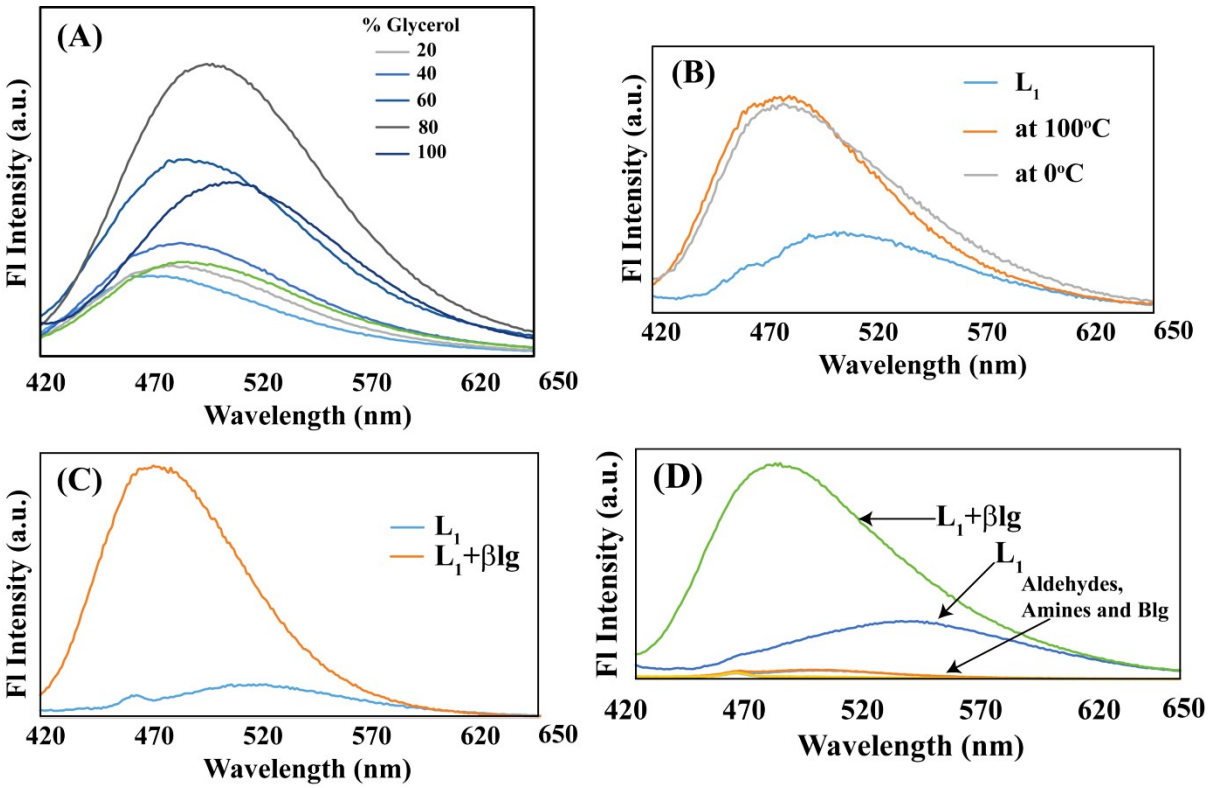

Figure S8: Emission spectra of **L_1** (10 μM) (A) with varying glycerol-ethanol percentage (B) displaying turn-on efficiency at extreme temperatures (C) Turn On efficiency at a concentration 1 μM with βlg (D) Interaction of βlg with starting materials and target compound.

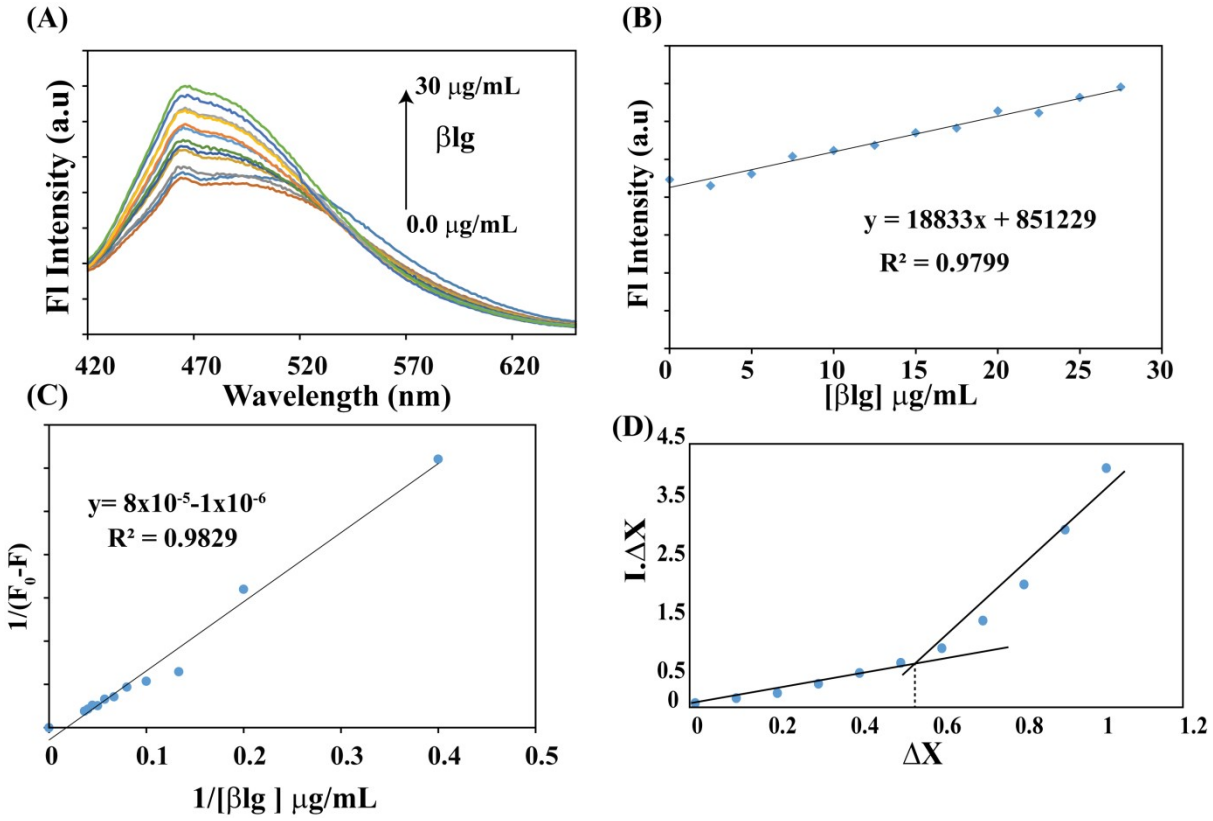

Figure S9: (A) Emission spectra of titration profile of gradual addition of βlg in buffered media to $\mathbf{L_1}$. (B) Determination of Limit of detection from titration. (C) Determination of binding constant. (D) Determination of stoichiometry from Job's Plot.

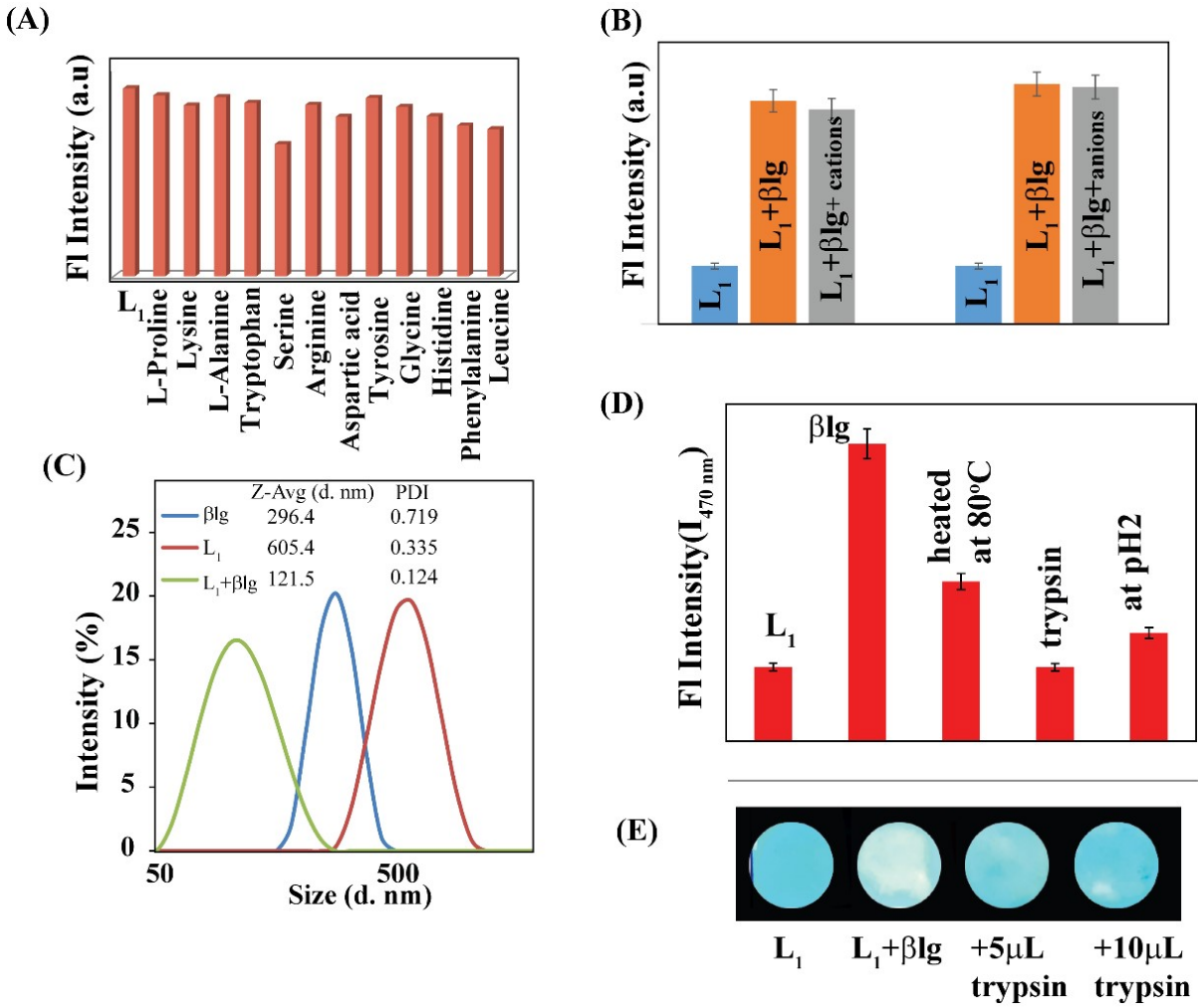

Figure S10: Bar diagram representing Fl intensity of $\mathbf{L_1}$ (10 μM) in buffered media (A) interacting with multiple amino acids (B) Turn-On emission signal in presence of biologically relevant cations (Na^+, K^+, Mg^{2+}, Ca^{2+}) and anions (F^-, Cl^-, Br^-, I^-). (C) DLS spectra of $\mathbf{L_1}$ and $\mathbf{L_1}$+βlg (D) Bar diagram of emission intensity of $\mathbf{L_1}$ and βlg in presence heat, low pH, and trypsin (E) Paper strips experiment held under UV-365 nm light, with varying concentrations of trypsin added to $\mathbf{L_1}$+βlg.

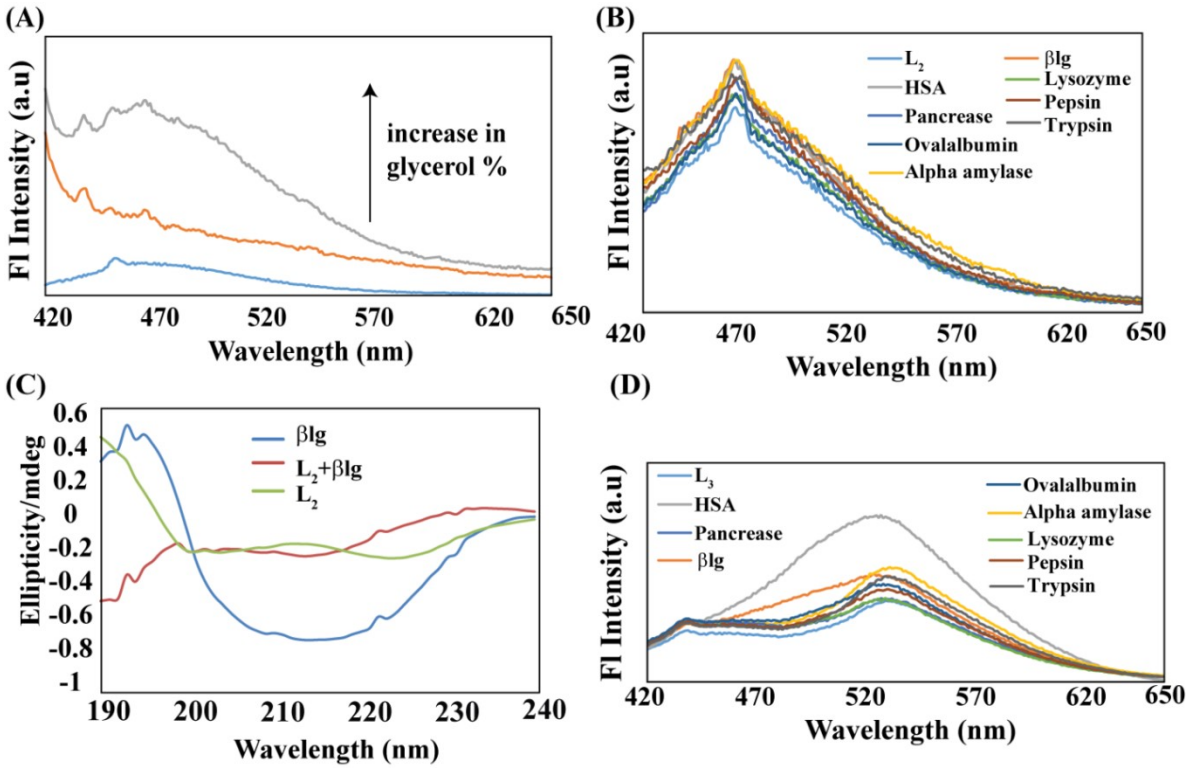

Figure S11: (A) Emission spectra of $\mathbf{L_2}$ (10 μM) with varying glycerol-ethanol percentage. (B) Emission spectra of $\mathbf{L_2}$ (10 μM) with various proteins and analytes in buffer media (C) CD spectra of $\mathbf{L_2}$ with targeted protein (D) Emission spectra of $\mathbf{L_3}$ (10 μM) with various proteins and analytes in buffer media

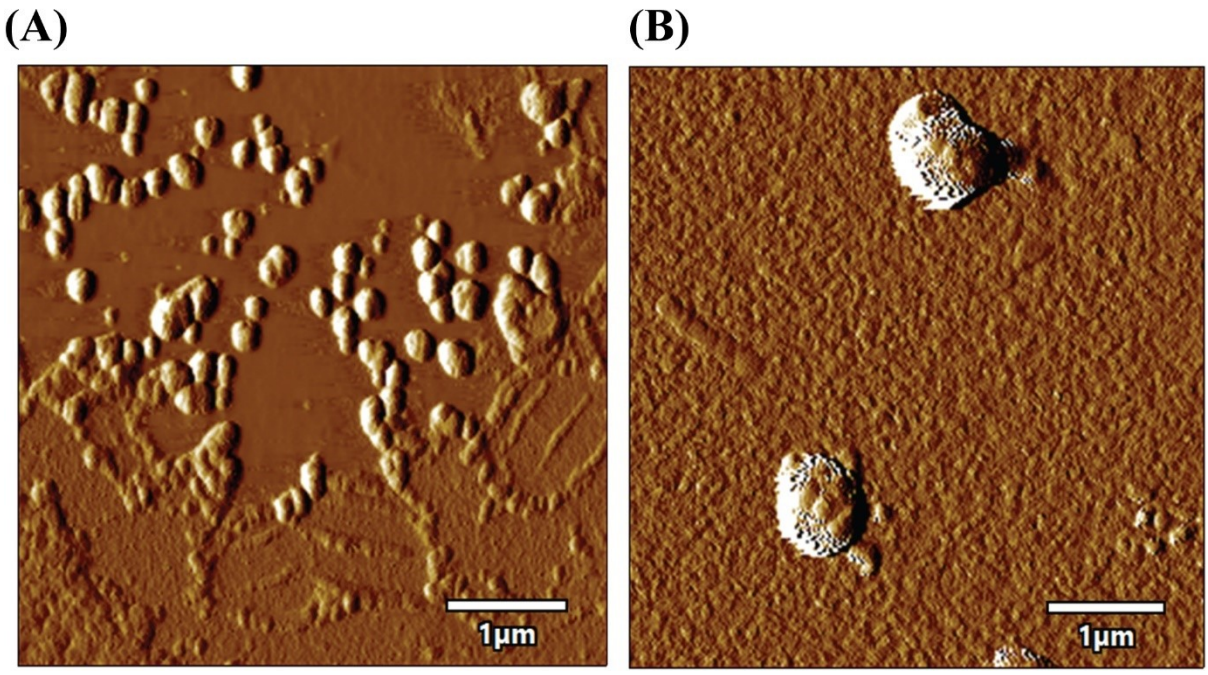

Figure S12: AFM of $\mathbf{L_2}$ (10 µM) (A) in 100% MeOH (B) 100% water

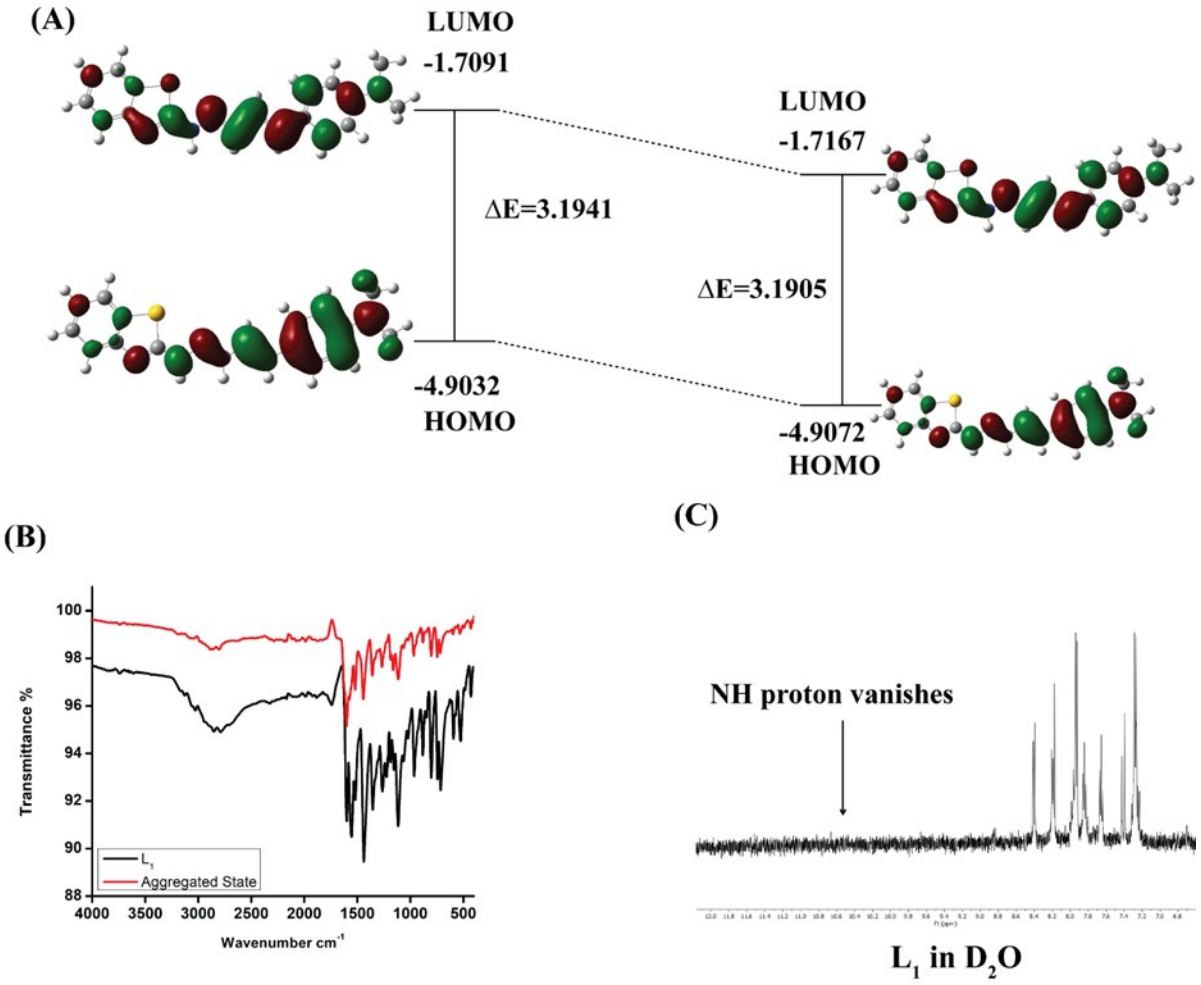

Figure S13: (A) DFT optimized structure of $\mathbf{L_1}$ in MeOH and Water. (B) IR spectra of $\mathbf{L_1}$ and aggregated state of $\mathbf{L_1}$. (C) ^{1}HMNR spectra of $\mathbf{L_1}$ taken in D_2O at room temperature.

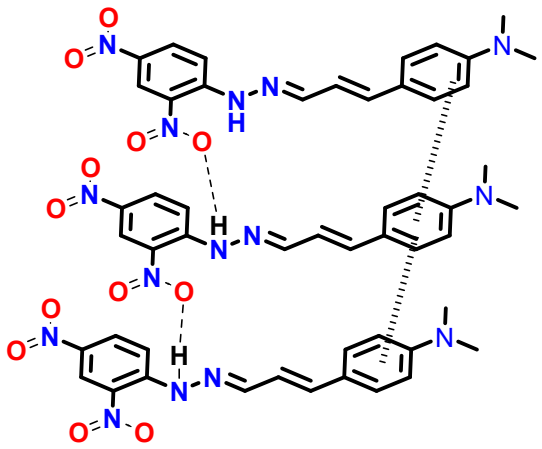

Figure S14: Probable aggregated structure of $\mathbf{L_2}$.

Table 1: A comparative layout of recent analytical methods for detecting β-lactoglobulin.

Sl no.	References	Mode of detection	LOD (ppm)
1.	This work	Synthetic probe via fluorescence detection	2.89
2	L. I. Boitz, G. Fiechter, R. K. Seifried and H. K. Mayer, J. Chromatogr. A, 2015, (1386), 98–102.	UPLC	7
3	L. P. Hong, M. F. Pan, X. Yang, X. Q. Xie, K. X. Liu, et al; 2022, 20(1), 51.	Molecularly imprinted fluorescence sensor	43
4.	J. Ji, P. Zhu, F. W. Pi, S. Chao, J. D. Sun, et al., 2017, (74), 79–88	Peptide-based LC-MRM/MS	200
5	A. J. Yang, K. F. Ji, M. F. Yang, Z. F. Li, Y. J. Xing, et al., 2021, 37(08), 333–339.	UPLC	20.41
6	J. Yang, Y. Zhang and Y. Lu, Anal. Methods, 2022, 14, 1872–1879	QD–Apt–GO fluorescence assay	0.09691
7	A. P. B. Clemente, H. Kuang, A.M. Shabana, T. P. Labuza, and E.Kokkoli, Bioconjugate Chem., 2019, 30, 11, 2763–2770	ELASA	0.18
8	J. Orcajo, M. Lavilla, I. Martínez-de-Marañón, *Anal. Chim. Acta*, 2019, 1052, 163-169.	ELISA	0.114

References

1. S. Ghosh, B. Roy and S. Bandyopadhyay, J. Org. Chem., 2019, 84, 12031−12039.
2. A. Rana, C. Gogoi, S. Ghosh, S. Nandi, S. Kumar, U. Manna and S. Biswas, New J. Chem., 2021,45, 20193-20200.
3. N. Borah, S. De, A. Gogoi and G. Das, New J. Chem., 2020, 44, 18703-18713.